Electronic Supplementary Information

Biomineralization-inspired Nanozyme for Single-Wavelength Laser Activated Photothermal-Photodynamic Synergistic Treatment Against Hypoxic Tumors

Pengping Xu[1§], Xueying Wang[2§], Tuanwei Li[1], Huihui Wu[2], Lingli Li[3], Zhaolin Chen[3], Lei Zhang[3], Zhen Guo[2*] and Qianwang Chen[1*]*

[1]Hefei National Laboratory for Physical Sciences at Microscale, Department of Materials Science & Engineering & Collaborative Innovation Center of Suzhou Nano Science and Technology, CAS High Magnetic Field Laboratory, University of Science and Technology of China, Hefei, 230026, China.

[2]Anhui Key Laboratory for Cellular Dynamics and Chemical Biology, School of Life Sciences, University of Science and Technology of China, Hefei, 230027, China.

[3]Department of Pharmacy, the First Affiliated Hospital of USTC, Division of Life Sciences and Medicine, University of Science and Technology of China, Hefei, Anhui, 230001, China.

[§]The authors contributed equally to this work.

Corresponding authors:

Qianwang Chen: cqw@ustc.edu.cn;

Zhen Guo: zhenguo@ustc.edu.cn;

Lei Zhang: 76zhanglei@163.com.

Experimental

Chemicals and Materials: All reagents were used as received without further purification. Bovine serum albumin (BSA) and 1,3-diphenylisobenzofuran (DPBF) were purchased from Sigma-Aldrich. Ruthenium trichloride hydrate ($RuCl_3 \cdot xH_2O$), sodium hydroxide (NaOH), dimethyl sulfoxide (DMSO), hydrogen peroxide (H_2O_2, 30% w.t.), fluorescein diacetate (FDA) were purchased from Sinopharm Chemical Reagent CO., Ltd. Fluorescein isothiocyanate (FITC) was purchased from J&K. $[Ru(dpp)_3]Cl_2$ was from Alfa aesar. Reactive Oxygen Species Assay Kits were from Beyotime (DCFH-DA, S0033). HIF-1α antibody was from Abcam Co., Ltd. Hypoxyprobe-1 plus kits were from Hypoxyprobe, Inc. Dulbecco's Modified Eagle Media (DMEM) were from Gibco. Cell proliferation assay kits were from Promega (CellTiter 96 AQueous One Solution, G3580). Dialysis bag (M.W.C.O. 14 kDa) and phosphate buffered saline (PBS) were from Sangon. Ultrafiltration centrifuge tubes (M.W.C.O. 10 kDa) were from Millipore.

Characterization: The nanoagent was characterized by a transmission electron microscope (JEOL JEM-2100F) with an accelerating voltage of 200 kV. UV-vis spectra were recorded with a Persee TU1810 spectrophotometer. The X-ray photoelectron spectroscopy (XPS) was acquired using the XPS spectrometer (Thermal Scientific Escalab 250Xi). The hydrodynamic size was measured at 25 °C with a Malvern Zetasizer. The circular dichroism (CD) spectrum was measured on Jasco-810.

Synthesis of RuO_2@BSA: RuO_2@BSA nanodots (**RB**) were prepared through a biomineralization strategy in an aqueous solution. Typically, an aqueous $RuCl_3 \cdot xH_2O$ solution (10 mg mL^{-1}, 1 mL), and a BSA aqueous solution (20 mg mL^{-1}, 5 mL) were mixed in a glass bottle with magnetic stirring. 2 minutes later, 0.5 mL NaOH solution (1.0 M) was added to adjust the pH of the solution to ~12. After 12-hour reaction in a water bath, the solution was dialyzed in deionized water for 24 hours to remove excess precursors. The RuO_2@BSA solution was stored in a refrigerator at 4 ^oC for further use.

Synthesis of RuO_2@BSA@IR-808-Br_2: Br-modified NIR photosensitizer (IR-808-Br_2, abbreviated as **IR**) was attached to the RB by simply adding IR in DMSO to the RB aqueous solution (2 mg IR vs 100 mg BSA). After mild stirred for 12 hours, the product was dialyzed for 24 hours in pure water. The ultrafiltration centrifuge tube (M.W.C.O. 10 kDa) was used to concentrate the RuO_2@BSA@IR-808-Br_2 (**RBIR**) to obtain a concentrated product to meet some experimental needs.

Photothermal Effect: 1 mL aqueous solution of RB, IR or RBIR was transferred to a quartz cuvette, followed by a NIR laser (1.0 W cm^{-2}, 808 nm) irradiation for 10 min. The temperature was measured with a digital thermometer**.** This method was also adopted to obtain temperature rise profiles of different concentrations of RBIR (2.5 μM, 5 μM, 10 μM, 20 μM IR equiv.). The photothermal conversion efficiency (η) was determined with the previously reported method.

Oxygen Generation Experiments: To investigate the capability of evolving oxygen with intracellular concentration of H_2O_2, 100 μM of H_2O_2 was incubated with RBIR (10 μg mL^{-1} Ru equiv.) in PBS, followed by measuring the dissolved O_2 concentration with an oxygen sensor (Ocean Optic, NeoFox). The continuous catalytic effect was verified by repetitive addition of 1.25 mM of H_2O_2 to the solution and ventilated with N_2, followed by measuring the O_2 concentration with the sensor. The temperature-dependent catalytic activity was determined by mixing RBIR and H_2O_2 at 25 ^oC and 40 ^oC, respectively.

Singlet Oxygen ($^1O_2$) Generation: 1,3-diphenylisobenzofuran (DPBF) was used for the detection of $^1O_2$ generation. In a typical process, 20 μL of a DPBF solution (1 mg mL^{-1}) was added to 2 mL PBS buffer containing RBIR (2 μM of IR). Then the mixture was irradiated with an 808 nm laser (200 mW cm^{-2}). For hypoxic conditions, the mixture of DPBF and RBIR was ventilated with N_2 for 15 min, and the mixture was sealed up immediately after the addition of H_2O_2 (100 μM). Then the mixture was kept for 10 min at 37 °C before exposed to 808 nm irradiation with a power density of 200 mW cm^{-2}. The characteristic UV-vis absorption spectrum of the DPBF was measured to determine the generation of singlet oxygen.

Cell Uptake of RBIR: 4T1 cells were seed in 24-well plates at a density of $1x10^5$. After incubation for 24 hours, the culture medium was replaced by fresh medium containing different concentration of FITC labeled RBIR (0, 0.5, 1.0, 2.5 and 5.0 μM IR equiv.).

The cells were collected (8 hours later) and washed three times with PBS before flow cytometry analysis. Time-dependent cell uptake experiments were performed with fixed RBIR concentrations of 2.5 μM and the co-culture time gradients were set at 1 h, 2 h, 4 h and 8 h.

Dark Toxicity and Phototoxicity of RBIR under Normoxia and Hypoxic Conditions: 4T1 cells were seed in 96-well plates at a density of 1×10^4 per well. After incubation for 24 hours, the culture medium was replaced by fresh medium containing RBIR at different concentrations (0.1 μM to 5.0 μM IR equiv.). The cells were incubated for 24 hours and tested for cell viability by standard MTS protocol. For the photo-induced cytotoxicity test, These concentrations (0.5, 1, 2, 3 and 5 μM IR equiv.) are selected and additional laser irradiation (808 nm, 1.0 W cm^{-2}, 10 min) was applied after adding RBIR for 6 hours. For the dark toxicity and phototoxicity of RBIR under hypoxic conditions, all experimental conditions were consistent except that a transparent hypoxic culture jar (filled with a composition of 1% O_2, 5% CO_2 and 94% N_2) was used.

Detection of Intracellular O_2 Generation: 4T1 cells were seeded on the glass Petri dish. Then, the cells in each group were incubated with PBS or RBIR (2.5 μM and 5.0 μM IR equiv.) under normal or hypoxic conditions for 6 hours. These hypoxic cells were incubated with $[Ru(dpp)_3]Cl_2$ at a concentration of 10 μg mL^{-1} in a hypoxic incubator for another 12 h, followed by rinsing with PBS three times to remove free

$[Ru(dpp)_3]Cl_2$ and the residual RBIR. The level of intracellular O_2 was evaluated by detecting the fluorescence of $[Ru(dpp)_3]^{2+}$ (λex = 450 nm, λem = 610 nm) by fluorescence microscope.

Immunofluorescence for Cellular Hypoxia: 4T1 cells were treated with different concentration of RBIR in normoxic (0 μM) or hypoxic (0, 2.5 μM and 5.0 μM IR equiv.). After that, cells were fixed with 1% paraformaldehyde (PFA) at 37 ºC for 10 min and permeabilized in 0.2% Triton X-100 for 1 min, washed three times with PBS. After blocking with 1% bovine serum albumin in PBS containing 0.05% Tween-20 at room temperature for 45 min, the fixed cells were incubated with primary antibodies against HIF-1α (Alexa Fluor® 488 Conjugate) in a humidified chamber at 4 °C overnight, followed by phalloidin (Rhodamine Conjugate) at room temperature for 1 h, and then washed three times. Images were captured by DeltaVision softWoRx software (Applied Precision) and processed by deconvolution and z-stack projection.

Western Blot: 4T1 cells were treated with different concentration of RBIR in normoxic (0 μM) or hypoxic (0, 2.5 μM and 5.0 μM IR equiv.). Then the cells were collected in 1× SDS-PAGE (sodium dodecyl sulphate-polyacrylamide gel electrophoresis) sample buffer and boiled for 5min, samples were subjected to SDS-PAGE on a 10% gel and transferred onto nitrocellulose membranes. The nitrocellulose membrane was probed by primary antibodies against HIF-1α (Abcam, Cambridge, MA, USA) for evaluating the degree of hypoxia and against tubulin for the loading control, and then with

horseradish peroxidase (HRP)-labeled secondary antibody. The HIF-1α level was monitored by enhanced chemiluminescence using Gel Doc system (Bio-Rad).

Live/Dead Cell Staining Assays: 4T1 cells were seed in 24-well plates and incubated for 24 hours in the dark before treatments. After co-cultured with RBIR (5 μM IR equiv.) for 6 hours, the cells were treated with or without laser irradiation for 10 minutes (1.0 W cm^{-2}, 808 nm). The cells were co-stained with fluorescein diacetate (FDA) and propidium iodide (PI) and observed with fluorescence microscope (Olympus, IX71).

Intracellular Reactive Oxygen Species (ROS) Staining Assays: To give a direct observation of intracellular reactive oxygen species, DCFH-DA staining assays were performed. Briefly, 4T1 cells were seed in 6-well plates and incubated for 24 hours in the dark before treatment. After cultured in RBIR-containing medium (5 μM IR equiv.) for 6 hours followed by 30-minute ROS probe (DCFH-DA, 10 μM) loading, the cells were treated with or without laser irradiation for 10 minutes (100 mW cm^{-2}, 808 nm). The cells were observed with fluorescence microscope (Olympus, IX71).

Animal Model: Female Balb/c mice were purchased from Beijing Vital River Laboratory Animal Technology Co., Ltd. All animal procedures were performed in accordance with the Guidelines for Care and Use of Laboratory Animal Center in University of Science and Technology of China (USTC) and experiments were approved by the Animal Ethics Committee of Laboratory Animal Center in USTC. To

develop the tumor model, 1×10^6 4T1 cells suspended in 100 μL PBS were subcutaneously injected into the right back of each mouse. The mice were used when tumor volume reached about 150 mm^3.

In vivo NIR Fluorescence Imaging: 4T1 tumor-bearing mice used to observe the *in vivo* NIR fluorescence imaging performance of RBIR. The images were obtained with a living fluorescence imaging system equipped with a gas anesthesia device (IVIS Spectrum, PerkinElmer, λex = 745 nm, λem = 840 nm). After the pre-injection images were obtained, the mice were intravenously injected with RBIR (2.5 mg kg^{-1} IR equiv.). The images were acquired sequentially 0.5 h, 1 h, 2 h, 6 h, 12 h and 24 h post-injection under same imaging conditions.

Immunohistochemical Staining: To assess the hypoxia after administration of RBIR in the tumor microenvironment, mice were i.v. injected with RBIR (2.5 mg kg^{-1} of IR, PBS treated mice were used as control). 24 hours later, pimonidazole hydrochloride (60 mg kg^{-1}) was intraperitoneally injected into the mice. After 90 min, the mice were euthanized and the subcutaneous tumors were collected for immunohistochemical staining. The protocol for immunohistochemical staining was performed under the guidance of the manufacturer's instructions for Hypoxyprobe-1 plus kit (Hypoxyprobe Inc.).

In Vivo Infrared Thermography: To assess the *in vivo* thermography capacity, RBIR

was injected intravenously to the 4T1 tumor-bearing mice at a dosage of 2.5 mg kg^{-1} (IR equiv.). 6 hours later, the tumors were irradiated with a NIR laser (1.0 W cm^{-2}, 808 nm) for 10 minutes. The body temperature of the mice was recorded by an infrared camera (ICI-7320) and the temperature of the tumor was read by the software.

In vivo Single-wavelength Laser Activated Phototherapy: When the tumor volume (the tumor volume was calculated according to the normal equation $V = W^2 \times L/2$ commonly used in previous reports) reached about 150 mm^3, 4T1 tumor-bearing mice were randomly divided into 6 groups (n = 5). They are: (**1**) PBS group (100 μL); (**2**) IR group (dose = 2.5 mg kg^{-1} IR equiv., 100 μL); (**3**) RBIR group (dose = 2.5 mg kg^{-1} IR equiv., 100 μL); (**4**) PBS+L (100uL, 808 nm, 1.0 W cm^{-2}, 10 min); (**5**) IR+L (dose = 2.5 mg kg^{-1} IR equiv., 808 nm, 1.0 W cm^{-2}, 10 min) and (**6**) RBIR+L (dose = 2.5 mg kg^{-1} IR equiv., 808 nm, 1.0 W cm^{-2}, 10 min), respectively. Tumor volume and bodyweight of the mice before and after treatment were measured using a caliper and an electronic balance, respectively. After 14-day observation and measurement, the tumor tissues from each mouse were collected, fixed, photographed and weighed to compare the tumor treatment outcomes.

Biodistribution: RBIR was intravenously injected into 4T1 tumor-bearing mice (n = 3) at the dose of 2.5 mg kg^{-1} of IR. 24 hours later, the mice were euthanized and main organs (heart, liver, spleen, lung and kidneys) and tumor were excised. The *ex vivo* fluorescence imaging was performed by a living imaging system (IVIS Spectrum,

PerkinElmer, λex = 745 nm, λem = 820 nm).

Hematology and Biochemistry Analysis: RBIR were intravenously injected into healthy mice while PBS treated mice were used as control. Two weeks later, the blood samples for hematology analysis were collected with anticoagulation tubes. To obtain serum samples required for biochemistry analysis, the blood of the mice was collected and centrifuged (3000 rpm, 5 min) in centrifuge tubes. Hematology analysis and biochemistry analysis were performed on an automated blood analyzer and an automated biochemistry analyzer, respectively.

Statistical Analysis: All experiments were repeated at least three times, and all the results were reported as the mean ± standard deviations (mean ± SD). Statistical analysis was performed using Student's t-test and $*P < 0.05$ was considered statistically significant.

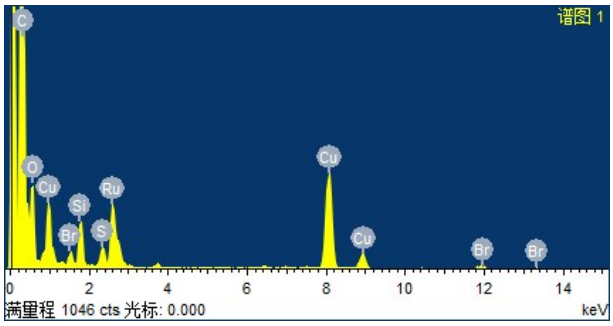

Figure S1. EDS result of RBIR (carbon film covered copper mesh was used as support).

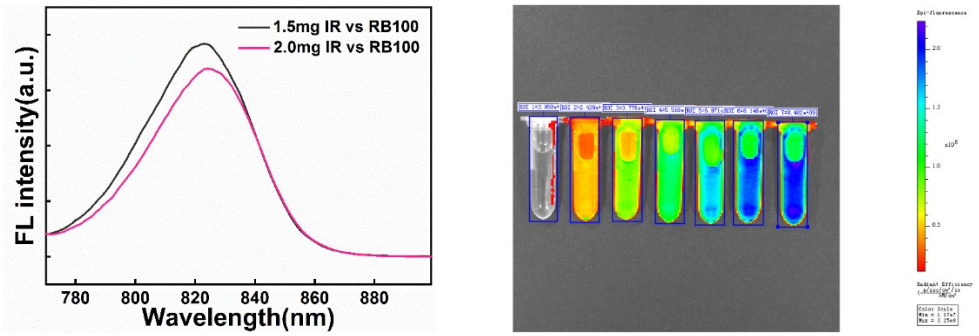

Figure S2. Fluorescence emission spectra of RBIR (left) and fluorescence imaging of RBIR in PBS (right).

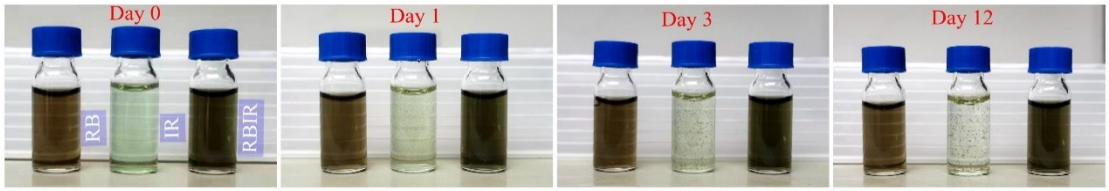

Figure S3. Photos of RB, IR, and RBIR in water at day 0, 1, 3, and 12. No precipitation and significant color change were observed in the RBIR aqueous solution.

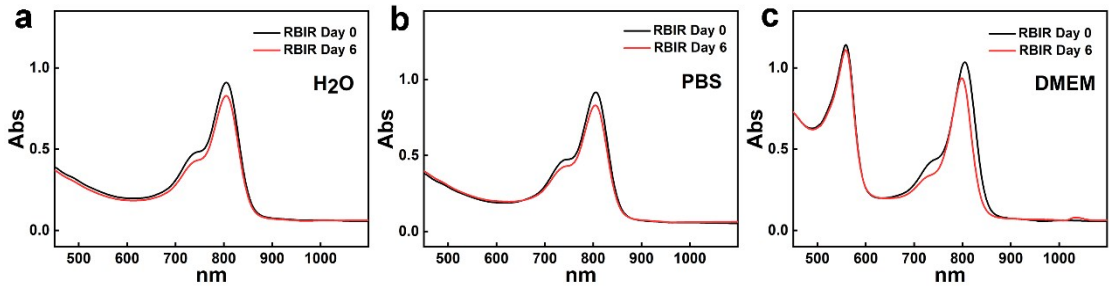

Figure S4. UV-vis absorption curves of RBIR in H_2O (**a**), PBS (**b**) and DMEM (**c**). After 6-day storage at 4 °C, the absorbance at the peak is attenuated by about 10%.

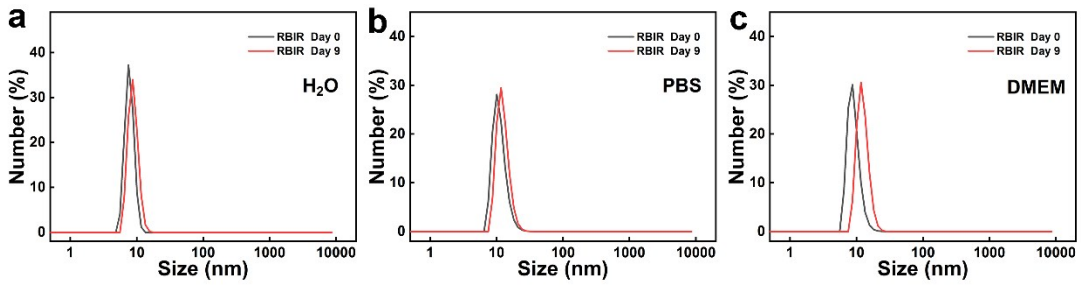

Figure S5. DLS profiles of RBIR in H2O (**a**), PBS (**b**) and DMEM (**c**) at day 0 and day 9. The particle size peak fluctuates in the range of 7.53 to 11.7 nm with no significant aggregation peak observed.

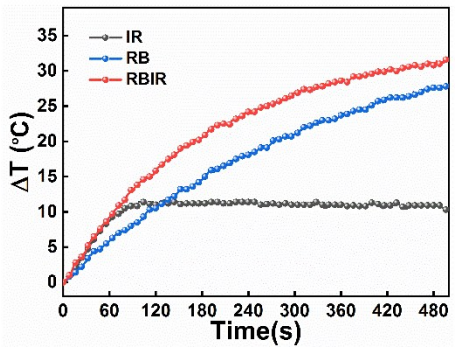

Figure S6. Photothermal effect of RB, IR and RBIR (808 nm, 1.0 W cm^{-2}). Both RB and IR contribute to the photothermal effect.

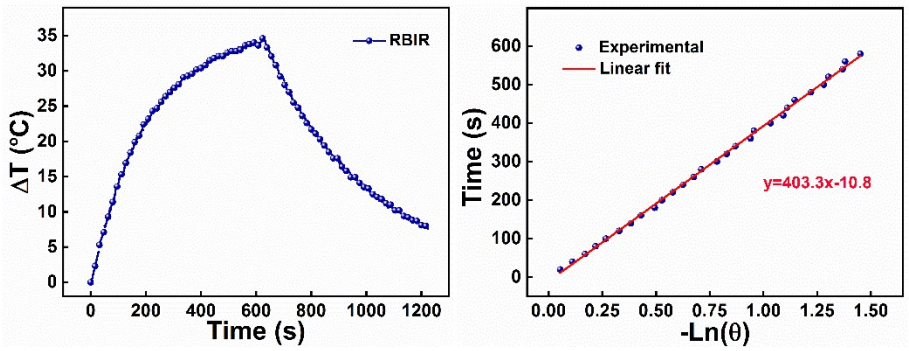

Figure S7. Photothermal conversion efficiency (η) measurement of RBIR and the η was calculated to be 33.6%. The detailed calculation is available at the end of this file.

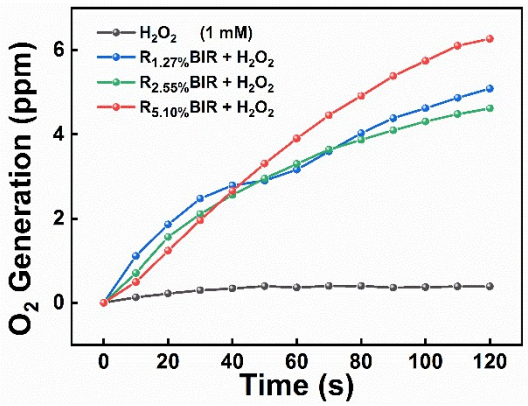

Figure S8. Catalase-like activity of RBIR with different RuO_2 to BSA mass ratios (1.27%, 2.55%, 5.10%). Results indicated that the difference in mass ratio of RuO_2 to BSA had a weak effect on catalytic activity when the amount of RuO_2 was consistent. This may be due to the RuO_2 produced by the biomineralization method was ultra-small in size and thus demonstrated extremely high catalytic performance.

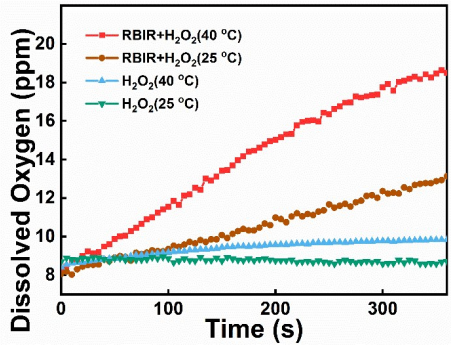

Figure S9. Catalytic activity of RBIR against H_2O_2 at 25 °C and 40 °C. Accelerated self-decomposition of H_2O_2 due to temperature rise is much lower than that on the catalytic decomposition process.

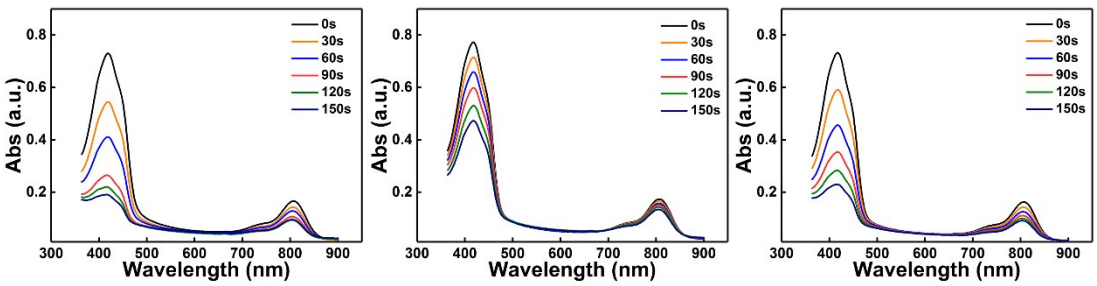

Figure S10. Singlet oxygen yield measurement using DPBF as indicator (from left to right: normoxia, hypoxia and hypoxia with 100 μM H_2O_2). Obviously, the

photodynamic efficiency of RBIR is suppressed by hypoxia. After the introduction of hydrogen peroxide, the photodynamic efficiency is restored.

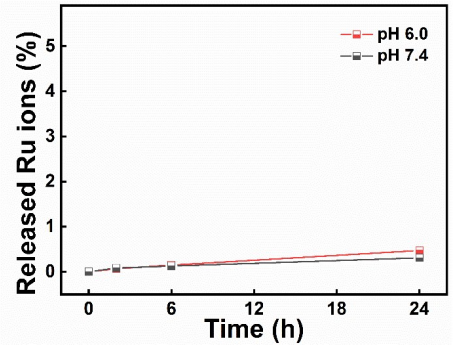

Figure S11. The Ru ions release profiles from RBIR in neutral (pH = 7.4) and acidic (pH = 6.0) PBS buffers. The RBIR shared closely similar release profiles in both neutral and acidic buffers (less than 0.5% at 24 hours), which is expected to avoid potential risk of ion leakage.

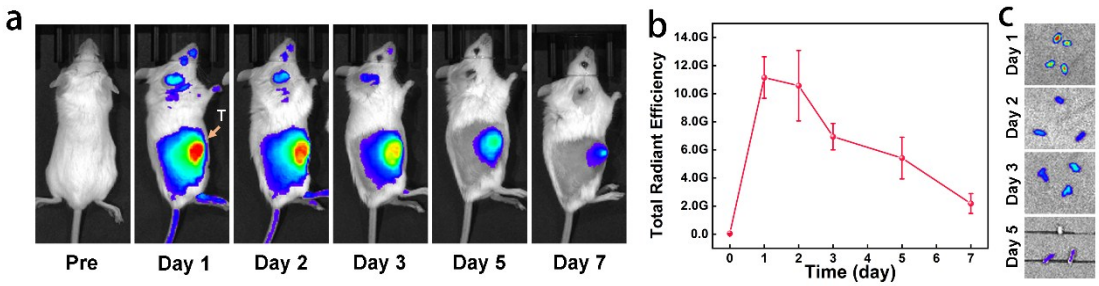

Figure S12. *In vivo* clearance investigation of RBIR after intravenous injection. **a)** Fluorescence images of mice before and after intravenous RBIR injection. **b)** Fluorescence intensity of selected region of interest. **c)** Feces of mice receiving RBIR injection.

Calculation of photothermal conversion efficiency (η):

The photothermal conversion efficiency of RBIR were calculated using the model described in Roper's et al. The equation is described as follows:

$$\sum_i m_i C_{p,i} \frac{dT}{dt} = Q_{NPs} + Q_{diss} - Q_{loss} \quad \text{----------(1)}$$

where m is the mass of the solution, C_p repsents the specific heat capacity of solvent (water), T is the solution temperature. Q_{NPs} is the photothermal energy absorbed by nanodots. Q_{diss} is the heat associated with the light absorbance of the solvent. Q_{loss} is thermal energy lost to the surroundings.

$$Q_{NPs} = I\left(1 - 10^{-A_{808}}\right)\eta \quad \text{----------(2)}$$

where η is the photothermal conversion efficiency. A_{808} is the absorbance intensity of nanodots at 808 nm. I is the power density of laser.

$$Q_{loss} = hS\Delta T \quad \text{----------(3)}$$

where h represents heat transfer coefficient. S is the surface area of the cuvette. ΔT is the temperature difference between the solution and the surroundings. When the system reaching an equilibrium temperature, dT/dt in equation (1) is 0. Then, $Q_{NPs} + Q_{diss} = Q_{loss} = hS\Delta T_{max}$, and we will get equation (4).

$$\eta = \frac{hS\Delta T_{max} - Q_{diss}}{I(1 - 10^{-A_{808}})} \quad \text{----------}$$

(4)

To calculate hS, θ which is defined as the ratio of ΔT to ΔT_{max} ($\Delta T/\Delta T_{max}$) is introduced. The equation (1) will be change to equation (5).

$$\frac{d\theta}{dt} = \frac{hS}{\sum_i m_i C_{p,i}}\left[\frac{Q_{NPs} + Q_{diss}}{hS\Delta T_{max}} - \theta\right] \quad \text{----------}$$

-(5)

When the laser was removed, the $Q_{NPs}+Q_{diss} = 0$, equation (5) will be changed to equation (6).

$$t = -\frac{\sum_i m_i C_{p,i}}{hS} ln\theta \quad \text{----------(6)}$$

where hS can be evaluated by plotting time as a function of –lnθ form the cooling curves.

For the RBIR, the ΔT_{max} is 34.6 ºC (ca. 26.2 - 60.8), Q_{diss} is measured independently to be 0.0243 J/s, I is 1.0 W cm^{-2} and A_{808} is 2.98. According to the linear time data versus –lnθ (**Figure S7**), and inputting approximate values for m (1 g) and C_p (4.2 J g^{-1} ºC^{-1})), the photothermal conversion efficiency of RBIR was calculated to be 33.6 %.